ORIGINAL ARTICLE

Air-Filled Substrate Integrated Waveguide for Smart Health Applications

Hidayah Mansor, Razi Abdul-Rahman

School of Mechanical Engineering, Universiti Sains Malaysia, 14300, Nibong Tebal, Malaysia

ABSTRACT

Introduction: For "smart health" Internet-of-Things (IoT) applications, substrate integrated waveguide (SIW) is a promising component to construct a wearable microwave device. For its efficacy in wearable devices, minimizing signal losses in terms of return and transition losses in SIW is of paramount importance. To enhance its performance, this paper presents the characterization of air-filled SIW transition losses for the SIW microwave device. **Method:** To investigate the effect of transition length on losses, the full-wave analysis of an air-filled SIW with different lengths of the taper transition was presented. For the analysis, the linear taper is designed for the Roger RT/Duroid 6002 substrate and utilized in the Ka-band frequencies. **Result:** From the full-wave analysis results, the length of the transition taper can be reduced considerably while achieving a wide-bandwidth characteristic of return loss better than 20 GHz. The results also show that the transmission loss can be reliably reduced while reducing the size of the SIW component. **Conclusion:** The findings may contribute to the development of the compact design of wearable microwave devices having a comparable performance with the conventional waveguide.

Keywords: Digital health, Wearable microwave device, Smart health Internet-of-Things (IoT) applications, Substrate integrated waveguide, Air-filled substrate integrated waveguide

Corresponding Author:
Hidayah Mansor, PhD
Email: menurhidayah@usm.my
Tel: +604-5996334

INTRODUCTION

Due to the demand for "smart health" Internet-of-Things (IoT) developments and systems, wearable microwave devices have gained popularity (1–3). The wearable device is one of the categories of digital health technologies that can be used to monitor, improve and organize health care resources (4). It is well-known that IoT applications need high-performance waveguide components to support high data rate communication links (5). Established printed guiding structures, e.g., microstrip, stripline, coplanar waveguide, etc., are generally accepted to exhibit high dielectric losses and become inefficient as a result of skin effect at high frequencies (6–7). Moreover, the rectangular waveguide is bulky and non-planar in nature (8). Hence, integrating and manufacturing at a low cost in the planar structure is difficult.

As a consequence, the substrate integrated waveguide (SIW) was utilized to customize printed flexible and high-performance wearable devices (9–10). SIW has many advantages compared to conventional rectangular waveguide (11–18). However, the main problem with the design of SIW components is to minimize the losses, especially when they include signal transitions (13). A widely accepted approach today to enhance the SIW performance is the use of air as the propagating medium to reduce losses and increase the capacity to handle power (19–22).

One of the more promising features of modified SIW is an air-filled substrate integrated waveguide (AFSIW) with a transition between the dielectric and the air-filled regions. Such a design has been proven to substantially improve losses, power handling capabilities and allows more flexibility for designing microwave devices (21). Nevertheless, the construction of a low-loss transition consisting of two types of material is difficult (23). In addition, any longer length of the transition will further increase the losses which can be observed from the values of the reflection and transmission coefficients (21). In fact, efforts have been focused to optimize the transition length for minimum losses as in (22–23). The achievement of the previous findings has conclusively shown that there exists a unique shape of the transition at a specific length that minimizes transition losses.

So far, the compact transition for modified SIW was introduced but it is well suited for Low-Temperature Cofired Ceramics (LTCC) technology (6). Hence, it is

of major interest to further minimize AFSIW losses at a shorter transition length to allow the possibility of the more compact design of printed SIW structure to achieve miniaturizations while enhancing the wearable microwave device performance. For that reason, the transition length effects on AFSIW structure losses are reported in this paper.

MATERIALS AND METHODS

To enable effective interconnection between dielectric- and air-filled in AFSIW circuits, a transition is suggested in (21). This transition is designed by using the characteristic equation (21). Based on the assessment in (24), the raised cosine taper is best suited for reducing the return and transmission losses throughout the transition. In this study, the linearly tapered transition is applied to characterize loss in dependence of transition length. For the transition taper design, the width of the taper W_1 increases with the distance t as

$$W_1(t)=a+(b-a)(t/L) \quad (1)$$

where the initial width a and the final width b of the transition taper are constants to ensure the transition continues. The design of the transition taper is shown in Fig. 1. Considering the height h is 0.508 mm, 20 different transition lengths L, i.e., 1 to 20 mm are used for data analysis. The choice for this range of transition lengths is in relation to the observation of the reflection coefficient (21). Referring to Figure 1, W_1 is the total width in the air-filled region, W is the width of the dielectric-filled SIW and W_2 is the width of the air-filled SIW. Taking into consideration the physical dimensions of the transitions in Table I, the transition from dielectric- to air-filled SIW is designed for the Roger RT/Duroid 6002 substrate ε_r in the Ka-band frequencies. Then, the full-wave analysis by using the high-frequency structural simulator (ANSYS HFSS) is applied to analyze an air-filled SIW transition structure. ANSYS HFSS is the industry standard for simulating 3-D full-wave electromagnetic fields. The steps of analysis are presented in Figure 2. As depicted

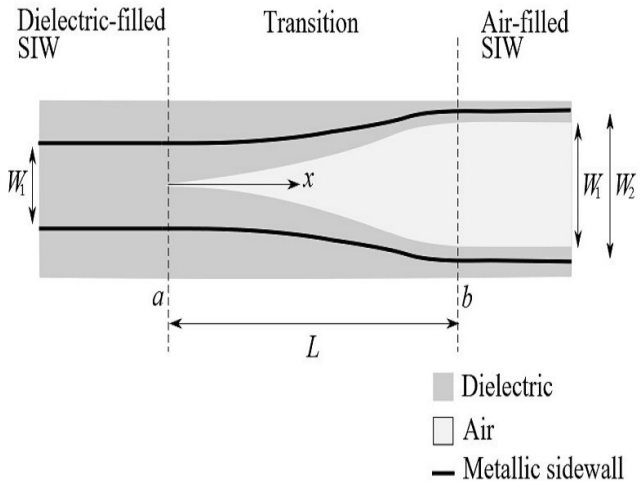

Figure 1: Design of the linearly tapered transition in HFSS

Table I: Structural properties of SIW

Band Freq.	Ka-band	
Parameters (mm)	AFSIW	SIW
W_1	7.02	
W_2	6	
W		4.12
ε_r	2.94	2.94
h	0.508	0.508

in Figure 1, the boundary of the top, bottom, and side surfaces are assigned as a perfect conductor. Then, the transition structure is divided into a finite element mesh using tetrahedral elements. For the wave port, W_1 is input port and W_2 is an output port in HFSS. The wave port acts as if there is a SMA connector is connected with SIW during the simulation. Before running the simulation, analysis of solution sweep and frequency needs to be pre-set before start simulation. After the simulation, the S-parameters results will be recorded. Based on S-parameters results, the return and transmission loss are observed and compared. The taper transition length with low losses is considered an effective transition taper design in terms of losses.

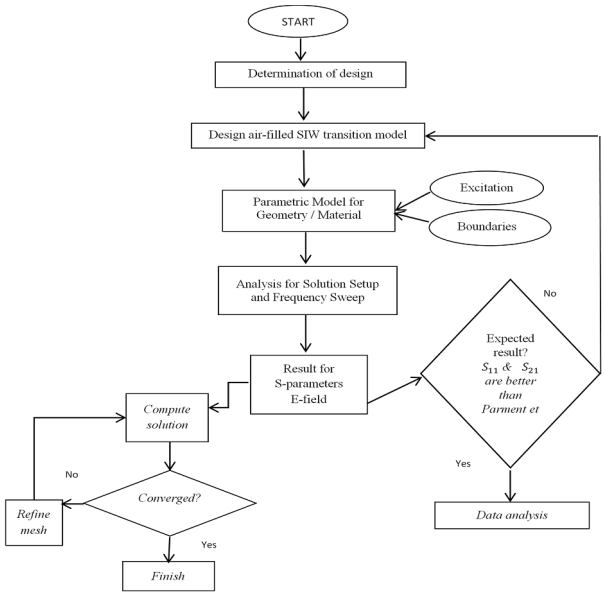

Figure 2: The steps of analysis

RESULTS

Figures 3 and 4 show the result of the reflection coefficient S_{11} of 1 to 20 mm transition length by a step size of 1 mm length. Based on the graph shown in Figure 3, the S_{11} of the 1 to 3 mm transition length signifies that air-filled SIW complete structure generates a high return loss. Thus it can be assumed that an incident wave is still reflected rapidly in the dielectric. The short transition and unmatched waves between dielectric- and air-filled are the reason for this incident wave. This phenomenon

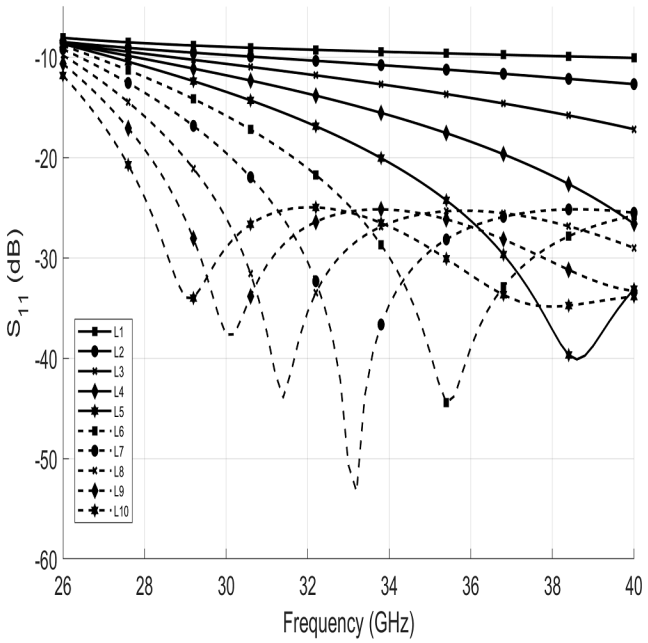

Figure 3: The reflection coefficient $|S_{11}|$ vs. 10 different transition lengths

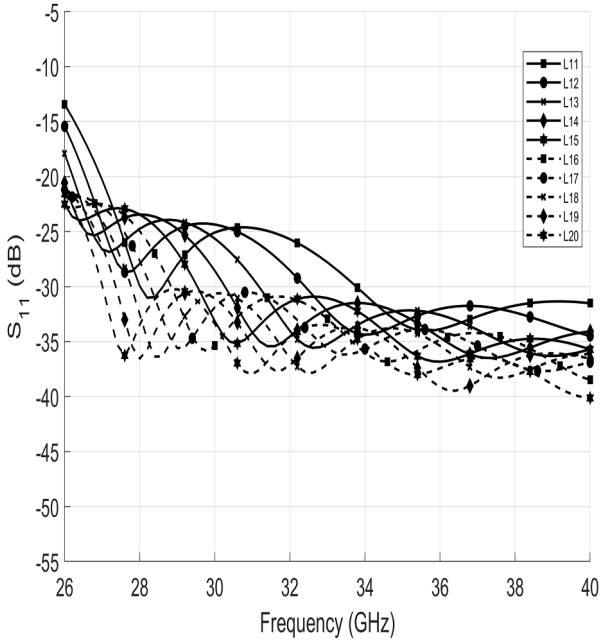

Figure 4: The reflection coefficient $|S_{11}|$ vs. 10 different transition lengths

is similar to a short-circuited transmission line (25). Starting at the 5 mm length, a dip of the S_{11} starts to occur within 37 to 40 GHz and the return loss better than 20 dB are obtained. As can be seen in Figure 3, the return loss is reduced slightly.

An increase in the transition length from 5 to 10 mm, as depicted in Figure 3, causes the single dip trend of the S_{11}. Based on this trend, the lower return loss may be noticed at a certain frequency. The 7 mm transition yields the lowest loss within this range. This corresponds to the reflection coefficient S_{11} at 33 GHz with a value of 54 dB. Nevertheless, it is still not deemed a well-designed transition as the bandwidth of return loss better than 20 dB within the frequency range of 30 to 40 GHz is not sufficiently wide for certain potential applications: E.g., an application with operating frequencies up to 30 GHz will experience return loss worse than 20 dB. The bandwidth of return loss better than 20 dB has been extended from 11 to 14 mm transition length as shown in Figure 4. As well as the transition length of 15 to 20 mm as depicted in Figure 4.

The transmission coefficient S_{21} results are shown in Figures 5 and 6. As can be seen in Figure 5, when the transition length increases, then S_{21} also decreases significantly. Therefore, the transmission of a wave from air to the electric medium is smooth. As a result,

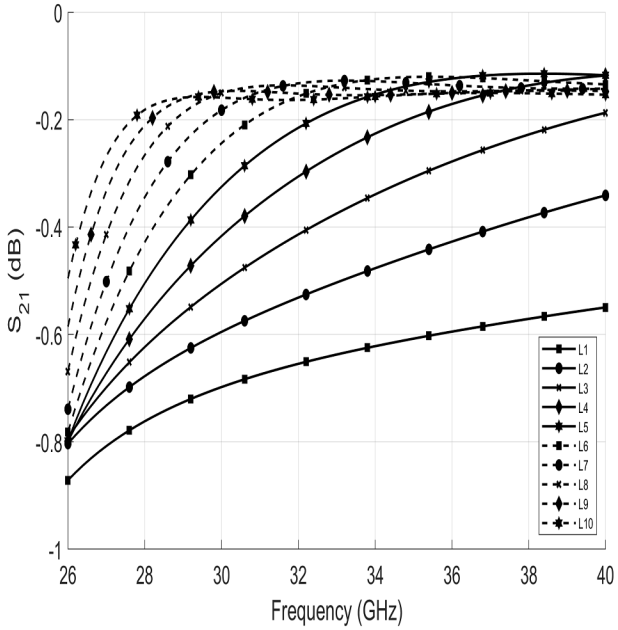

Figure 5: The reflection coefficient $|S_{21}|$ vs. 10 different transition lengths

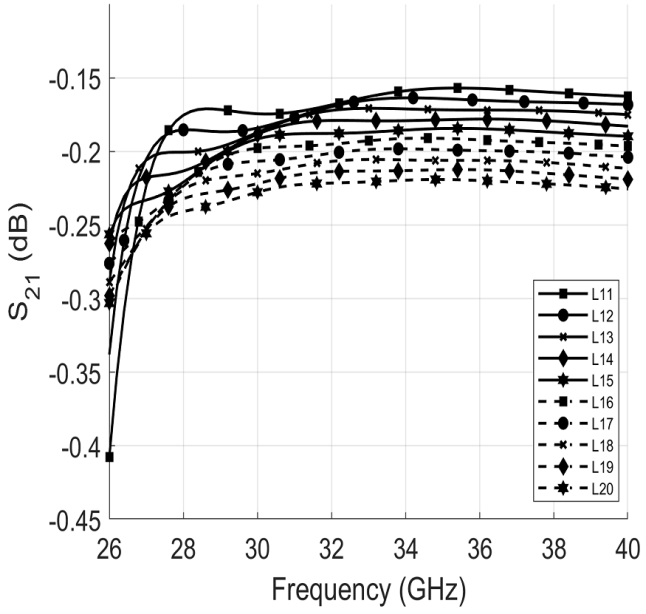

Figure 6: The reflection coefficient $|S_{21}|$ vs. 10 different transition lengths

the transmission loss is decreased. Starting at 11 mm transition length the S_{21} values increase as presented in Figure 6.

DISCUSSION

The full-wave analysis of an air-filled SIW transition as shown in Figure 1 with numerous different lengths of the transition is performed as an initial study to characterize the effect of transition length on losses. As shown in Figures 3 and 4, the values of the S_{11} drop at certain frequencies. This is because of the resonances and this situation has been reported in (26). Moreover, the resonant frequencies can be controlled by the transition (27). The relationship between resonant and the transition length can be seen in all figures. Based on Figure 3, 33 GHz is a higher resonant frequency for a 4 mm transition length, but at 7 mm transition length, it becomes a lower resonant frequency. Hence, an increase in the length causes the change in resonant frequency and an increase in the bandwidth of return loss better than 20 dB.

In contrast, the transmission loss increases slowly due to the resonance when the length of the transition is increased from 11 to 20 mm as shown in Figures 5 and 6. Therefore, an increment in the transition length causes an increment in the bandwidth of return loss better than 20 dB, which suggests that a wide-bandwidth for the Ka-band can be achieved by increasing the transition length. Unfortunately, this also effectively increases the transition loss. As such, the bandwidth and transmission loss are in a trade-off relationship.

CONCLUSION

To increase an air-filled SIW transition performance, both the return and transition losses along the transition need to be minimized. For this purpose, the losses along the transition have been characterized by using full-wave analysis. The results of the full-wave analyses have shown important characteristics of the losses in the transition that are beneficial in the design of SIW. The linear transition, which is the simplest design, is quite effective for the length of 10 mm onwards for Ka-bands. The results from the full-wave analysis have conclusively shown that the length of the taper can be used to control the transition losses. This paper contributes to the existing research in air-filled SIW transition design whereby under the right geometry of the transition structure, the transition length can be minimized to achieve miniaturization while maintaining the optimum quality of signal transmission. The contribution of the findings is to develop a compact design of the wearable microwave device with better performance compared to the conventional waveguide.

ACKNOWLEDGEMENT

This research is being funded by USM grant 304/PMEKANIK/6315404.

REFERENCES

1. Caccami MC, Mulla MYS, Natale CD, Marrocco G. Graphene oxide-based radio frequency identification wearable sensor for breath monitoring. IET Microwaves, Antennas & Propagation. 2018; 12(4): 467-471.
2. Benito-Lopez F, Coyle FS, Byrne R, Diamond D. Sensing sweat in real-time using wearable microfluidics. In: Proceedings of the 7th International Workshop on Wearable and Implantable Body Sensor Networks, Singapore; 2010.
3. Su W, Cook BS, Tentzeris MM. Additively manufactured microfluidics-based "peel-and-replace" RF sensors for wearable applications. IEEE Transactions on Microwave Theory and Techniques.2016; 64(6): 1928–1936.
4. Christian J, Dasgupta N, Jordan M, Juneja M, Nilsen W, Reites J. Digital Health and Patient Registries: Today, Tomorrow, and the Future.3rd ed. Addendum: AHRQ; 2018.
5. Nguyen NH, Parment F, Ghiotto A, Wu K, Vuong TP. A Fifth-Order Air-filled SIW Filter For Future 5G Applications. In: MTT-S International Microwave Workshop Series on Advanced Materials and Processes, 20-22 September 2017, Pavia, Italy: IEEE; 2017.
6. Isapour A, Kouki AB. Empty LTCC Integrated Waveguide with Compact Transitions for Ultra-Low Loss Millimeter-wave Applications. IEEE Microwave and Wireless Components Letters. 2017; 27(2):144-146.
7. Cheng DK. Field and Wave Electromagnetics. Canada: Addison- Wesley Publishing Company; 1989.
8. Kumar H, Jadhav R, Ranade S. A Review on Substrate Integrated Waveguide and its Microstrip Interconnect. IOSR Journal of Electronics and Communication Engineering. 2012; 3(5): 36–40.
9. Moro R, Agneessens S, Rogier H, Bozzi M. Circularly-polarised cavity-backed wearable antenna in SIW technology. IET Microwaves, Antennas & Propagation. 2018; 12(1); 127-131.
10. Su W, Wu Z, Fang Y, Bahr R, Raj PM, Tummala R, et al. 3D Printed Wearable Flexible SIW and Microfluidics Sensors for Internet of Things and Smart Health Applications. In: IEEE MTT-S International Microwave Symposium (IMS), 4-9 June 2017, Honolulu, HI, USA: IEEE.544-547; 2017.

11. Deslandes D, Wu K. Integrated Microstrip and Rectangular Waveguide in Planar Form. IEEE Microwave and Wireless Compon. Lett. 2001; 11(2): 68-70.
12. Deslandes D, Wu K. Single-substrate integration technique of planar circuits and waveguide filters. IEEE Transactions on Microwave Theory and Techniques. 2003; 51(2): 593-596. DOI:10.1109/tmtt.2002.807820
13. Bozzi M, Perregrini L, Wu K, Arcioni P. Current and Future Research Trends in Substrate Integrated Waveguide Technology. Radioengineering.2009; 18 (2): 201-209
14. Bozzi M, Winkler SA, Wu K. Broadband and compact ridge substrate integrated waveguides. IET Microwaves, Antennas & Propagation. 2010;4(11):1965. DOI:10.1049/iet-map.2009.0529.
15. Cassivi Y, Perregrini L, Arcioni P, Bressan M, Wu K, Conciauro G, (2002). Dispersion Characteristic of Substrate Integrated Rectangular Waveguide. IEEE Microw. Wireless Compon. Lett. 2002; 12(9):333-334. DOI:10.1109/LMWC.2002.803188.
16. Ng Mou Kehn M. Modal Analysis of Substrate Integrated Waveguides with Rectangular Via-Holes Using Cavity and Multilayer Green's Functions. IEEE Transactions on Microwave Theory and Techniques. 2014; 62(10):2214-2231. DOI:10.1109/tmtt.2014.2344626
17. Xu F, Wu K. Guided-wave and leakage characteristics of substrate integrated waveguide. IEEE Transactions on Microwave Theory and Techniques. 2005; 53(1): 66–73. DOI:10.1109/TMTT.2004.839303.
18. Lai Q, Fumeaux C, Hong W, Vahldieck R. Characterization of the Propagation Properties of the Half-Mode Substrate Integrated Waveguide. IEEE Transactions on Microwave Theory and Techniques. 2009; 57(8): 1996-2004
19. Ranjkesh N, Shahabadi M. Loss Mechanisms in Siw and Msiw. Progress in Electromagnetics Research B.2008; 42(21): 299–309.
20. Jin L, Lee RMA, Robertson I. Analysis and Design of a Novel Low-Loss Hollow Substrate Integrated Waveguide. IEEE Transactions on Microwave Theory and Techniques. 2014; 62(8): 1616-1624. DOI:10.1109/tmtt.2014.2328555.
21. Parment F, Ghiotto A, Vuong TP, Duchamp JM, Wu K. Air- Filled Substrate Integrated Waveguide for Low-Loss and High Power- Handling Millimeter-Wave Substrate Integrated Circuits. IEEE Transactions on Microwave Theory and Techniques. 2015;63(4):1228-1238. DOI:10.1109/tmtt.2015.2408593.
22. Belenguer A, Esteban H, Boria VE. Novel Empty Substrate Integrated Waveguide for High-Performance Microwave Integrated Circuits. IEEE Transactions on Microwave Theory and Techniques.2014; 62(4): 832- 839.
23. Ghassemi N, Boudreau I, Deslandes D, Wu K. Millimeter-Wave Broadband Transition of Substrate Integrated Waveguide on High- to-Low Dielectric Constant Substrates. IEEE Transactions on Components, Packaging and Manufacturing Technology. 2013; 3(10): 1764- 1770. DOI:10.1109/tcpmt.2013.2257929.
24. Mansor H, Abdul Rahman R. Optimal transition in Air-filled Substrate Integrated Waveguide. In: Research and Development (SCOReD), 2015 IEEE Student Conference on, 13-14 Dec. 2015, Kuala Lumpur, Malaysia: IEEE. 20016;172-176.
25. Kraus JD, Fleisch DA. Electromagnetics with Applications.Singapore: McGraw-Hill Book Co.P; 1999.
26. Kushta T, Narita K, Kaneko T, Saeki T, Tohya H. Resonance Stub Effect in a Transition from a Through Via Hole to a Stripline in Multilayer PCBs. IEEE Microwave and Wireless Components Letters. 2003;13(5): 169-171.
27. A.J. Theiss. Measuring Return-Loss Resonances to Estimate RF Wall Loss in MM-Wave Coupled-Cavity Circuits. IEEE Transactions on Electron Devices. 2009; 56(5): 981-985.